

# Modeling and Energy Optimization of LDPC Decoder Circuits with Timing Violations

François Leduc-Primeau, Frank R. Kschischang, and Warren J. Gross

## Abstract

This paper proposes a quasi-synchronous design approach for signal processing circuits, in which timing violations are permitted, but without the need for a hardware compensation mechanism. The error-correction performance of low-density parity-check (LDPC) code ensembles is evaluated using density evolution while taking into account the effect of timing faults, and a method for accurately modeling the effect of faults at a high level of abstraction is presented. Following this, several quasi-synchronous LDPC decoder circuits are designed based on the offset min-sum algorithm, providing a 23%–40% reduction in energy consumption or energy-delay product, while achieving the same performance and occupying the same area as conventional synchronous circuits.

## I. INTRODUCTION

The time required for a signal to propagate through a CMOS circuit varies depending on several factors. Some of the variation results from physical limitations: the delay depends on the initial and final charge state of the circuit. Other variations are due to the difficulty (or impossibility) of controlling the fabrication process and the operating conditions of the circuit [1]. As process technologies approach atomic scales, the magnitude of these variations is increasing, and reducing the supply voltage to save energy increases the variations even further [2].

The variation in propagation delay is a source of energy-inefficiency for synchronous circuits, and new design approaches have been proposed to tackle this. In *better than worst-case* (BTWC)

F. Leduc-Primeau and W. J. Gross are with the Department of Electrical and Computer Engineering, McGill University, Montreal, Canada (e-mail: francois.leduc-primeau@mail.mcgill.ca, warren.gross@mcgill.ca). F. R. Kschischang is with the Department of Electrical and Computer Engineering, University of Toronto, Toronto, Canada (e-mail: frank@ece.utoronto.ca).

A preliminary version of this work was presented at the IEEE ICC 2015 conference.

[3] or *voltage over-scaled* (VOS) circuits, efficiency is improved by allowing some timing violations to occur, while including a mechanism to compensate or recover from these faults. One such method consists in introducing special latches that can detect timing violations, and to restart the circuit when a violation is detected [4], [5]. Since the circuit’s latency is increased significantly when a timing violation occurs, this approach is only suitable for tolerating small fault rates (e.g.  $10^{-7}$ ) and for applications where the circuit can be easily restarted, such as speculative microprocessors. In the case of signal processing circuits, we are usually interested in the average quality of the output, which creates more possibilities for dealing with timing violations. A seminal contribution in this area was the algorithmic noise tolerance (ANT) approach [6], [7], which is to allow timing violations to occur in the main processing block, while adding a separate reliable processing block with reduced precision that is used to bound the error of the main block, and provide algorithmic performance guarantees. The downside of the ANT approach is that it relies on the assumption that timing violations will first occur in the most significant bits. If that is not the case, the precision of the circuit could degrade to the precision of the auxiliary block, limiting the scheme’s usefulness. For many circuits, including some adder circuits [8], this assumption does not hold. Furthermore, the addition of the reduced precision block and of a comparison circuit increases the area requirement.

We propose a general design methodology for digital circuits with a relaxed synchronicity requirement that does not rely on any hardware compensation mechanism. Instead, we provide performance guarantees by re-analyzing the algorithm while taking into account the effect of timing violations. We call such circuits *quasi-synchronous* circuits.

We use the quasi-synchronous approach to design energy-optimized low-density parity-check (LDPC) decoder circuits based on a state-of-the-art soft-input algorithm and architecture. LDPC decoding algorithms are good candidates for a quasi-synchronous implementation because their throughput and energy consumption are limiting factors in many applications, and like other signal processing algorithms, their performance is determined by the average quality of their output. Furthermore, we show that the iterative nature of the decoding algorithm allows for additional energy savings.

The topic of unreliable LDPC decoders has been discussed in a number of contributions. Varshney studied the Gallager-A and the Sum-Product decoding algorithms when the computations and the message exchanges are “noisy”, and showed that the density evolution analysis

still applies [9]. The Gallager-B algorithm was also analyzed under various scenarios [10]–[12]. A model for an unreliable quantized Min-Sum decoder was proposed in [13], which provided numerical evaluation of the density evolution equations as well as simulations of a finite-length decoder. The quantized Min-Sum decoder was also analyzed in [14] for the case where faults are the result of storing decoder messages in an unreliable memory. None of these contributions make an explicit link between the reliability of the computation and the energy consumed by the decoder.

In this paper, we present a circuit design framework that captures the effect of timing violations caused by a reduced supply voltage and increased clock frequency, while simultaneously measuring the energy consumption. We show that the information provided by the framework can be used as part of a density evolution analysis to evaluate the channel threshold and iterative performance of the decoder when affected by timing faults. To perform density evolution, we propose an accurate high-level model for the effect of timing faults, which is also suitable for algorithm-level simulations of finite-length decoders. Finally, we show that under mild assumptions, the problem of minimizing the energy consumption of a quasi-synchronous decoder can be simplified to the energy minimization of a small test circuit, and present an approximate optimization method similar to Gear-Shift Decoding [15] that finds sequences of quasi-synchronous decoders that minimize decoding energy.

The remainder of the paper is organized as follows. Section II reviews LDPC codes and describes the circuit architecture of the decoder that is used to measure timing faults. Section III presents the *deviation* model that represents the effect of timing faults on the algorithm. Section IV then discusses the use of the density evolution method to predict the performance of a decoder affected by timing faults. Finally, Section V presents the energy optimization strategy and results, and Section VI concludes the paper. Additional details on the CAD framework used for circuit measurements can be found in Appendix A, and Appendix B provides some details concerning the simulation of the test circuits.

## II. LDPC DECODING ALGORITHM AND ARCHITECTURE

### A. Code and Channel

We consider a communication scenario where a sequence of information bits is encoded using a binary LDPC code of length  $n$ . The LDPC code is described by an  $m \times n$  binary parity-check

matrix  $H$ , or equivalently by a factor graph composed of *variable* nodes indexed from 1 to  $n$  and of *check* nodes indexed from 1 to  $m$ . For the  $H$  matrix and the graph to represent the same code, the graph must contain an edge between a variable node  $i$  and a check node  $j$  if and only if the element of  $H$  at row  $j$  and column  $i$  is non-zero. We assume that the LDPC code is regular, and denote the degree of variable nodes by  $d_v$ , and the degree of check nodes by  $d_c$ .

Let us assume that the transmission takes place over the Additive White Gaussian Noise (AWGN) channel. A codeword  $\mathbf{x} \in \{-1, 1\}^n$  is transmitted through the channel, which outputs the received vector  $\mathbf{y} = \mathbf{x} + \mathbf{W}$ , where  $\mathbf{W}$  is a vector of  $n$  independent and identically distributed zero-mean normal random variables with variance  $\sigma_w^2$ . The AWGN channel has the property of being output symmetric, meaning that  $\mathbb{P}(y_i = q|x_i = 1) = \mathbb{P}(y_i = -q|x_i = -1)$ .

Let the *belief* output  $\mu_i$  of the channel be given by

$$\mu_i = \frac{\alpha y_i}{\sigma_w^2}, \quad (1)$$

with  $\alpha > 0$ . Note that if  $\alpha = 2$  then  $\mu_i$  is in the log-likelihood ratio format. Assuming that  $x_i = 1$  was transmitted, then  $\mu_i$  has a normal distribution with mean  $\alpha/\sigma_w^2$  and variance  $\alpha^2/\sigma_w^2$ , and therefore when  $\alpha$  is fixed, its distribution can be described by a single parameter  $\rho = \alpha/\sigma_w^2$ , yielding  $\mu_i \sim \mathcal{N}(\rho, \alpha\rho)$ . We call this distribution a one-dimensional (1-D) normal distribution. The distribution of  $\mu_i$  can also be specified using other equivalent parameters, such as the probability of error  $p_e$ , given by

$$p_e = \mathbb{P}(\mu_i < 0|x_i = 1) = \mathbb{P}(\mu_i > 0|x_i = -1) = \frac{1}{2} \operatorname{erfc}\left(\frac{1}{\sqrt{2\sigma_w^2}}\right) = \frac{1}{2} \operatorname{erfc}\left(\sqrt{\frac{\rho}{2\alpha}}\right), \quad (2)$$

where  $\operatorname{erfc}(\cdot)$  is the complementary error function.

## B. Algorithm

The well-known Offset Min-Sum (OMS) algorithm is a simplified version of the Sum-Product algorithm that can usually achieve similar error-correction performance. It has been widely used in implementations of LDPC decoders [16]–[18]. To make our decoder implementation more realistic and show the flexibility of our design framework, we present an algorithm and architecture that support a row-layered message-passing schedule. Architectures optimized for this schedule have proven effective for achieving efficient implementations of LDPC decoders [17]–[19]. Using a row-layered schedule also allows to pipeline the decoder to increase the

circuit's utilization. In a row-layered LDPC decoder, the rows of the parity-check matrix are partitioned into  $L$  sets called *layers*. We assume that all the columns in a given layer contain at most one non-zero element, which enables some architectural simplifications. Note that as a result,  $L \geq d_v$ .

Using the equivalent graph representation of the code, a layer with index  $\ell$  can be defined as a set  $\mathcal{L}_\ell$  of check nodes,  $\ell \in [1, L]$ . In a given iteration, each variable node (VN) receives at most one message for each layer, and the inputs of a given VN can share the same index variable as the layers. Let  $\mu_i^{(t,\ell)}$  be the message sent by a VN  $i$  to its neighboring check node in layer  $\ell$  during iteration  $t$ , and  $\lambda_i^{(t,\ell)}$  be the belief message received by VN  $i$  after evaluating layer  $\ell$  during iteration  $t$ . Note that messages sent from variable nodes can also be uniquely identified by specifying the iteration index  $t$ , the VN index  $i$ , and the index  $j$  of the check node receiving the message, leading to the notation  $\mu_{i,j}^{(t)}$ . We use the second notation when we want to avoid specifying the type of message-passing schedule being used. Finally, we denote the channel information corresponding to the  $i$ -th codeword bit by  $\mu_i^{(0)}$ , since it also corresponds to the first message sent by a variable node  $i$  to all its neighboring check nodes.

The Offset Min-Sum algorithm used with a row-layered message-passing schedule is described in Algorithm 1. In the algorithm,  $v_i$  represents the VN with index  $i$ ,  $\mathcal{N}(c)$  denotes the set of VNs that are neighbors of a check node  $c$ , and  $\Lambda_i^{(t,\ell)}$  represents the current sum of incoming messages at a VN  $i$ . At all times we have that

$$\Lambda_i^{(t,\ell')} = \mu_i^{(0)} + \sum_{\ell=1}^{\ell'} \lambda_i^{(t,\ell)}, \quad 1 \leq \ell' \leq L. \quad (3)$$

The check node (CN) function  $\text{CHK}(S)$  is defined as follows. Define a set  $S$  of VN-to-CN messages as  $S = \{\mu_1, \mu_2, \dots, \mu_{d_c-1}\}$ . Then

$$\text{CHK}(S) = \max \left( 0, \min_{\mu_i \in S} |\mu_i| - C \right) \cdot \prod_{\mu_i \in S} \text{sign}(\mu_i), \quad (4)$$

where  $C \geq 0$  is the offset parameter, and

$$\text{sign}(x) = \begin{cases} 1 & \text{if } x \geq 0, \\ -1 & \text{if } x < 0. \end{cases}$$

---

**Algorithm 1: Offset Min-Sum algorithm with a row-layered message-passing schedule.**


---

**input** :  $\{\mu_1^{(0)}, \mu_2^{(0)}, \dots, \mu_n^{(0)}\}, T$   
**output**:  $\{\hat{x}_1, \hat{x}_2, \dots, \hat{x}_n\}$

```

1 begin
    // Initialization
2  $\Lambda_i^{(0,0)} \leftarrow \mu_i^{(0)}, \forall i \in [1, n]$ 
3  $\lambda_i^{(0,\ell)} \leftarrow 0, \forall i \in [1, n], \ell \in [1, L]$ 
    // Decoding
4 for  $t \leftarrow 1$  to  $T$  do
5     for  $\ell \leftarrow 1$  to  $L$  do
        // VN to CN messages
6         if  $\ell = 1$  then
7              $\mu_i^{(t,\ell)} \leftarrow \Lambda_i^{(t-1,L)} - \lambda_i^{(t-1,\ell)}, \forall i$ 
8         else
9              $\mu_i^{(t,\ell)} \leftarrow \Lambda_i^{(t,\ell-1)} - \lambda_i^{(t-1,\ell)}, \forall i$ 
        // CN to VN messages
10        for  $c \in \mathcal{L}_\ell$  do
11            for  $i \in \{i : v_i \in \mathcal{N}(c)\}$  do
12                 $\lambda_i^{t,\ell} \leftarrow \text{CHK}(\{\mu_k^{(t,\ell)} : v_k \in \mathcal{N}(c) \setminus \{v_i\}\})$ 
        // VN update
13         $\Lambda_i^{(t,\ell)} \leftarrow \mu_i^{(t,\ell)} + \lambda_i^{(t,\ell)}, \forall i$ 
14         $\forall i : \hat{x}_i \leftarrow 1$  if  $\Lambda_i^{(t,\ell)} \geq 0, \hat{x}_i \leftarrow -1$  if  $\Lambda_i^{(t,\ell)} < 0$ 

```

---

### C. Architecture

The factor graph of the code can also be used to represent the computations that must be performed by the decoder. At each decoding iteration, one message is sent from variable to check nodes on every edge of the graph, and again from check to variable nodes. We call a variable node processor (VNP) a circuit block that is responsible for generating messages sent by a given variable node, and similarly a check node processor (CNP) a circuit block generating messages sent by a given check node.

In a row-layered architecture in which the column weight of layer subsets is at most 1, there is at most one message to be sent and received for each variable node in a given layer. Therefore

VNPs are responsible for sending and receiving one message per clock cycle. CNPs on the other hand receive and send  $d_c$  messages per clock cycle. At any given time, every VNP and CNP is mapped respectively to a VN and a CN in the factor graph. The routing of messages from VNP to CNPs and back can be posed as two equivalent problems. One can fix the mapping of VNs to VNP and of CNs to CNPs, and find a permutation of the message sequence that matches VNP outputs to CNP inputs, and another permutation that matches CNP outputs to VNP inputs. Alternatively, if VNP process only one message at a time, one can fix the connections between VNP and CNPs, and choose the assignment of VN to VNP to achieve correct message routing. We choose the later approach because it allows studying the computation circuit without being concerned by the routing of messages.

The number of CNPs instantiated in the decoder can be adjusted based on throughput requirements from 1 to  $m/L$  (the number of rows in a layer). As the number of CNPs is varied, the number of VNP will vary from  $d_c$  to  $n$ . An architecture diagram showing one VNP and one CNP is shown in Fig. 1. In reality, a CNP is connected to  $d_c - 1$  additional VNP, which are not shown. The memories storing the belief totals  $\Lambda_i^{(t,\ell)}$  and the intrinsic beliefs  $\lambda_i^{(t,\ell)}$  are also not shown. The part of the VNP responsible for sending a message to the CNP is called VNP *front* and the part responsible for processing a message received from a CNP is called the VNP *back*. The VNP front and back do not have to be simultaneously mapped to the same VN. This allows to easily vary the number of pipeline stages in the VNP and CNPs. Fig. 1 shows the circuit with two pipeline stages.

Messages exchanged in the decoder are fixed-point numbers. The position of the binary point does not have an impact on the algorithm, and therefore the messages sent by VNs in the first iteration can be defined as rounding the result of (1) to the nearest integer, while choosing a suitable  $\alpha$ . The number of bits in the quantization, the scaling factor  $\alpha$ , and the OMS offset parameter are chosen based on a density evolution analysis of the reliable algorithm (described in Section IV). We quantize decoder messages on 6 bits, which allows a reliable decoder to have approximately the same channel threshold as a floating-point decoder.

In order to analyze a circuit that is representative of state-of-the-art architectures, we use an optimized architecture for finding the first two minima in each CNP. Our architecture is inspired by the “tree structure” approach presented in [20], but requires fewer comparators. Each pair of CNP inputs is first sorted using the *Sort* block shown in Fig. 2a. These sorted pairs are

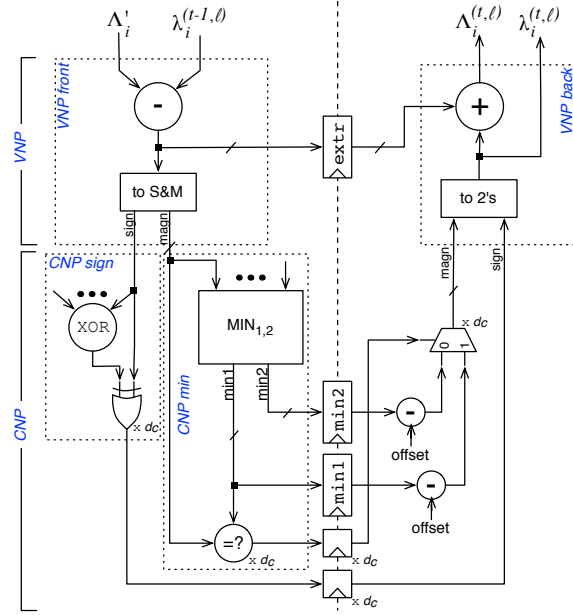


Fig. 1. Block diagram of the layered Offset Min-Sum decoder architecture.

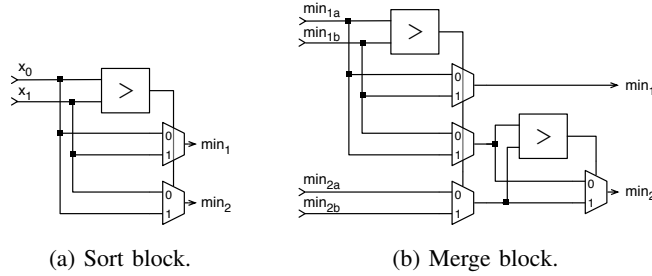


Fig. 2. Logic blocks used in the  $MIN_{1,2}$  unit.

then merged recursively using a tree of *Merge* blocks, shown in Fig. 2b. If the number of CNP inputs is odd, the input that cannot be paired is fed directly into a special merge block with 3 inputs, which can be obtained from the 4-input *Merge* block by removing the  $min_{2b}$  input and the bottom multiplexer.

Note that it is possible that changes to the architecture could increase or decrease the robustness of the decoder (see e.g. [21]), but this is outside the scope of this paper.

### III. DEVIATION MODEL

#### A. Quasi-Synchronous Circuit Design

We consider synchronous circuits that permit timing violations without hardware compensation, resulting in what we call *quasi-synchronous* circuits. Optimizing the energy consumption of these circuits requires an accurate model of the impact of timing violations, and of the energy consumption. We propose to achieve this by characterizing one or several *test circuits* that are subsets of the complete circuit implementation.

The term *deviation* refers to the effect of circuit faults on the result of a computation, and the deviation model is the bridge between the circuit characterization and the analysis of the algorithm. We reserve the term *error* for describing the algorithm, in the present case to refer to the incorrect detection of a transmitted symbol.

We are interested in modeling deviations occurring in a synchronous circuit, and therefore the computation can be represented as a discrete-time system. In a deviation-free context, the circuit accepts an input  $X[t]$  at time  $t \in \{0, 1, 2, \dots\}$  and outputs a result  $Y[t]$ . Note that the circuit could require one or several clock cycles to generate  $Y[t]$ , but this is irrelevant to the characterization of the computation. When operated in a quasi-synchronous manner, the circuit instead outputs  $Z[t]$ , which is a corrupted version of  $Y[t]$ . From the point of view of the algorithm analysis, it is convenient to model deviations on  $Y[t]$  as a transmission through a memoryless communication channel, where the deviation  $D[t]$  corresponds to additive noise, such that  $Z[t] = Y[t] + D[t]$ . However, it is challenging to generate simple and accurate descriptions of the deviation  $D[t]$ . The main difficulty is that the propagation delay through the circuit depends on its internal charge state and therefore on previous inputs. To address this, we assume that  $X[t]$ ,  $Y[t]$ , and  $D[t]$  can be modeled as stationary random processes. This allows us to use a Monte-Carlo simulation to measure the probability distribution of  $Z[t]$  or  $D[t]$ . To alleviate the restriction imposed by the stationarity assumption, we can characterize the circuit for several distributions of  $X[t]$ .

We are interested in using the test circuit to characterize not only deviations, but also energy consumption. Both deviations and energy depend on the choice of some design parameters. Let  $\Gamma$  be the space of design parameters that we are considering. For a probability distribution of  $X[t]$  parametrized by  $\pi$  and system parameters  $\gamma \in \Gamma$ , we define a function  $f_\gamma(\pi)$  that provides a parametrization of the distribution of  $Z[t]$ , and a function  $c_\gamma(\pi)$  that provides the average

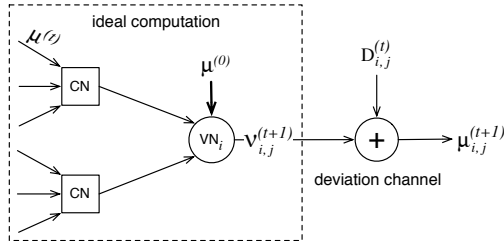


Fig. 3. Computation tree of an LDPC decoder combined with the deviation model (for a regular LDPC code with  $d_c = 4$  and  $d_v = 3$ ).

energy consumed by the circuit to produce one output.

### B. Deviation Model

In LDPC decoding, the smallest unit of computation consists in evaluating the one-iteration computation tree, shown within the dashed box in Fig. 3, in the sense that the state of the decoder remains unchanged unless all the computations required to update the computation tree are performed. Furthermore, all the computations performed in an LDPC decoder can be represented in terms of this computation tree, and therefore the computation tree constitutes a good basis for the test circuit, on which deviations will be measured.

There are  $(d_v - 1)$  check nodes in the tree. Each of these check nodes receives  $(d_c - 1)$  messages from neighboring variable nodes, and generates a message sent to the one VN whose message was excluded from the computation. This VN then generates the ideal extrinsic message based on the messages received from neighboring check nodes and on the channel prior  $\mu^{(0)}$ . Let  $\nu_{i,j}^{(t+1)}$  be the message that would be sent from variable node  $i$  to check node  $j$  during iteration  $t + 1$  if no deviations had occurred during iteration  $t$ .

As discussed in Section III-A, we propose to model all the deviations that have occurred during the computation of  $\nu_{i,j}^{(t+1)}$  by considering that the ideal output of the computation is transmitted through an additive-noise communication channel. This is shown in Fig. 3, where a deviation  $D_{i,j}^{(t)}$  is added to the output of iteration  $t$ . For the first messages sent in the decoder at  $t = 0$ , deviations cannot occur, and therefore we simply have  $\mu_{i,j}^{(0)} = \nu_{i,j}^{(0)}$ .

We now want to define the statistical properties of  $D_{i,j}^{(t)}$  to represent the behavior of the circuit as accurately as possible. We know that deviations caused by timing violations depend

on the current and past inputs to a combinational circuit. A first step in simplifying the model would be to instead assume that the deviation depends on the current and past *outputs* of the circuit. However, at the algorithm level, the mapping of circuit to computations is not known, and therefore it is difficult to know what the previous output of the circuit was. It is however always known what the current ideal output is, and therefore it is possible to construct a deviation model that depends on  $\nu_{i,j}^{(t+1)}$ . This was done in [22], where deviations are modeled by specifying the conditional probability distribution of  $\mu_{i,j}^{(t+1)}$  given  $\nu_{i,j}^{(t+1)}$ . However, such a model does not allow capturing the dependency of deviations on the previous states of the circuit. To include this dependency in the model, we propose to have it also depend on other quantities that are available at the algorithm level and that provide information on the statistics of state transitions in the circuit. For this, we use the value of the transmitted bit  $x_i$ , and the message error probability at the beginning of the iteration  $p_e^{(t)}$ , defined as

$$p_e^{(t)} = \mathbb{P}\left(\mu_{i,j}^{(t)} < 0 \mid x_i = 1\right) + (1/2) \cdot \mathbb{P}\left(\mu_{i,j}^{(t)} = 0\right). \quad (5)$$

We denote the probability distribution of a random variable  $\mu$  by  $\phi_\mu(x)$ , and the conditional probability distribution of  $\mu$  given  $\nu$  by  $\phi_{\mu|\nu}(x|y)$ , or simply  $\phi(\mu|\nu)$ . The proposed deviation model is described by a set of probability distributions  $\phi^{(p_e^{(t)})}(\mu_{i,j}^{(t+1)}|\nu_{i,j}^{(t+1)}, x_i)$ , indexed by the message error probability  $p_e^{(t)}$ . Equivalently, the model can be described by the set of deviation distributions  $\phi^{(p_e^{(t)})}(D_{i,j}^{(t)}|\nu_{i,j}^{(t+1)}, x_i)$ . Note that the deviation channel remains memoryless, since  $x_i$  is constant throughout the decoding, and  $p_e^{(t)}$  does not depend on the particular messages sent in the decoder.

#### IV. PERFORMANCE ANALYSIS

##### A. Standard Analysis Methods for LDPC Decoders

Density evolution (DE) is the most common tool used for predicting the error-correction performance of an LDPC decoder. The analysis relies on the assumption that messages passed in the factor graph are mutually independent, which holds as the code length goes to infinity [23]. Given the channel output probability distribution and the probability distribution of variable node to check node messages at the start of an iteration, DE computes the updated distribution of variable node to check node messages at the end of the decoding iteration. This computation can be performed iteratively to determine the message distribution after any number of decoding

iterations. The validity of the analysis rests on two properties of the LDPC decoder. The first property is the conditional independence of errors, which states that the error-correction performance of the decoder is independent from the particular codeword that was transmitted. The second property states that the error-correction performance of a particular LDPC code concentrates around the performance measured on a cycle-free graph, as the code length goes to infinity.

Both properties were shown to hold in the context of reliable implementations [23]. It was also shown that the conditional independence of errors always holds when the channel is output symmetric and the decoder has a symmetry property. We can define a sufficient symmetry property of the decoder in terms of a message-update function  $F_{i,j}$  that represents one complete iteration of the (ideal) decoding algorithm. Given a vector of all the messages  $\boldsymbol{\mu}^{(t)}$  sent from variable nodes to check nodes at the start of iteration  $t$  and the channel information  $\nu_i^{(0)}$  associated with variable node  $i$ ,  $F_{i,j}$  returns the next ideal message to be sent from a variable node  $i$  to a check node  $j$ :  $\nu_{i,j}^{(t+1)} = F_{i,j}(\boldsymbol{\mu}^{(t)}, \nu_i^{(0)})$ .

**Definition 1.** A message-update function  $F_{i,j}$  is said to be symmetric with respect to a code  $C$  if

$$F_{i,j}(\boldsymbol{\mu}^{(t)}, \nu_i^{(0)}) = x_i F_{i,j}(\mathbf{x}\boldsymbol{\mu}^{(t)}, x_i \nu_i^{(0)})$$

for any  $\boldsymbol{\mu}^{(t)}$ , any  $\nu_i^{(0)}$ , and any codeword  $\mathbf{x} \in C$ .

In other words, a decoder's message-update function is symmetric if multiplying all the belief messages in the decoder by a valid codeword  $\mathbf{x}$  only affects the sign of the VN-to-CN messages, and if additionally the sign of a message sent by a VN  $i$  is flipped if and only if  $x_i = -1$ . Note that the symmetry condition in Definition 1 is implied by the check node and variable node symmetry conditions in [23, Def. 1].

### B. Applicability of Density Evolution

In order to use density evolution to predict the performance of long finite-length codes, the decoder must satisfy the two properties stated in Section IV-A, namely the conditional independence of errors and the convergence to the cycle-free case. Our approach for modeling the deviations is to first measure the deviation statistics directly on gate-level circuit models

using Monte-Carlo simulations. Within that context, the lack of an analytical model makes it impossible to establish with certainty that the conditional independence of errors still applies when the decoder is affected by deviations. However, we perform measurements on the test circuits both using all-one codewords and using random codewords and obtain similar results even when deviations occur.

We now show that the conditional independence of errors and the convergence to the cycle-free case can be satisfied when deviations in the decoder occur according to the model presented in Section III-B.

Let  $\mathbf{x} \in \{-1, 1\}^n$  be the transmitted codeword, and let  $\mathbf{y}$  denote the channel output. The channel can be modeled multiplicatively as  $y_k = x_k z_k$  ( $k \in [1, n]$ ), where  $\{z_k\}$  is a sequence of independent and identically distributed (i.i.d.) random variables that represent the channel noise. In a reliable decoder, messages are completely determined by the received vector  $\mathbf{xz}$ , but in a faulty decoder, there is additional randomness that results from the deviations. Therefore, we represent messages in terms of conditional probability distributions given  $\mathbf{xz}$ .

**Definition 2.** We say that a message distribution  $\phi_{\mu_{i,j}^{(t)}}(\mu|\mathbf{xz})$  is symmetric if

$$\phi_{\mu_{i,j}^{(t)}}\left(\mu_{i,j}^{(t)}|\mathbf{xz}\right) = \phi_{\mu_{i,j}^{(t)}}\left(x_i\mu_{i,j}^{(t)}|\mathbf{z}\right).$$

The probability of a message error given in (5) can also be written as  $\mathbb{P}\left(x_i\mu_{i,j}^{(t)} < 0\right) + (1/2) \cdot \mathbb{P}\left(\mu_{i,j}^{(t)} = 0\right)$ . Note that if a message has a symmetric distribution, its error probability is the same whether  $\mathbf{xz}$  or  $\mathbf{z}$  is received, since  $\mathbf{y} = \mathbf{z}$  implies that  $x_i = 1$ .

Similarly to the results presented in [22], we can show that the symmetry of message distributions is preserved when the message-update function is symmetric.

**Lemma 1.** If  $F_{i,j}$  is a symmetric message-update function and if  $\nu_i^{(0)}$  and  $\mu_{i,j}^{(t)}$  have symmetric distributions for all  $(i, j)$ , the next ideal messages  $\nu_{i,j}^{(t+1)}$  also have symmetric distributions.

*Proof:* Using the fact that  $\phi_{\nu_i^{(0)}}\left(\nu_i^{(0)}|x_i z_i\right) = \phi_{\nu_i^{(0)}}\left(x_i \nu_i^{(0)}|z_i\right)$ , the distribution of the next ideal message can be expressed as

$$\phi_{\nu_{i,j}^{(t+1)}}\left(\nu_{i,j}^{(t+1)}|\mathbf{xz}\right) = \int_{\mathbb{R}^n} F_{i,j}\left(\boldsymbol{\mu}^{(t)}, \nu_i^{(0)}\right) \phi_{\boldsymbol{\mu}^{(t)}}\left(\boldsymbol{\mu}^{(t)}|\mathbf{xz}\right) \phi_{\nu_i^{(0)}}\left(x_i \nu_i^{(0)}|z_i\right) d\boldsymbol{\mu}^{(t)} d\nu_i^{(0)}. \quad (6)$$

Since the graph is cycle-free and  $\mu_{i,j}^{(t)}$  has a symmetric distribution for all  $(i, j)$ , we have

$$\phi_{\boldsymbol{\mu}^{(t)}}(\boldsymbol{\mu}^{(t)}|\mathbf{xz}) = \prod_k \phi_{\mu_k^{(t)}}(\mu_k^{(t)}|\mathbf{xz}) = \prod_k \phi_{\mu_k^{(t)}}(x_k \mu_k^{(t)}|\mathbf{z}), \quad (7)$$

where  $\mu_k^{(t)}$  are the elements of  $\boldsymbol{\mu}^{(t)}$ . We let  $\boldsymbol{\mu}' = \mathbf{x}\boldsymbol{\mu}^{(t)}$  and  $\nu'_i = x_i \nu_i^{(0)}$ . Using (7) and the fact that the message-update function is symmetric, (6) becomes

$$\begin{aligned} \phi_{\nu_{i,j}^{(t+1)}}(\nu_{i,j}^{(t+1)}|\mathbf{xz}) &= \int_{\mathbb{R}^n} x_i F_{i,j}(\boldsymbol{\mu}', \nu'_i) \prod_k \phi_{\mu_k^{(t)}}(\mu_k^{(t)}|\mathbf{z}) \phi_{\nu_i^{(0)}}(\nu'_i|z_i) d\boldsymbol{\mu}' d\nu'_i \\ &= \int_{\mathbb{R}^n} x_i F_{i,j}(\boldsymbol{\mu}', \nu'_i) \phi_{\boldsymbol{\mu}^{(t)}}(\boldsymbol{\mu}'|\mathbf{z}) \phi_{\nu_i^{(0)}}(\nu'_i|z_i) d\boldsymbol{\mu}' d\nu'_i \\ &= \phi_{\nu_{i,j}^{(t+1)}}(x_i \nu_{i,j}^{(t+1)}|\mathbf{z}), \end{aligned}$$

and therefore the next ideal messages have a symmetric distribution.  $\blacksquare$

To establish the conditional independence of errors under the proposed deviation model, we first define some properties of the deviation.

**Definition 3.** We say that a deviation random variable  $D_{i,j}^{(t)}$  is symmetric if

$$\phi_{D_{i,j}^{(t)}}(d|\mathbf{xz}) = \phi_{D_{i,j}^{(t)}}(-d|\mathbf{xz}).$$

**Definition 4.** We say that a deviation random variable  $D_{i,j}^{(t)}$  is weakly symmetric if there exists a random variable  $\Delta_{i,j}^{(t)}$  with the same sample space as  $D_{i,j}^{(t)}$  and independent of  $\mathbf{x}$  such that

$$\phi_{D_{i,j}^{(t)}}(d|\mathbf{xz}) = \phi_{\Delta_{i,j}^{(t)}}(x_i d|\mathbf{z}).$$

Note that if  $D_{i,j}^{(t)}$  satisfies the symmetry condition, it also satisfies the weak symmetry condition (by choosing  $\Delta_{i,j}^{(t)}$  such that  $\phi_{\Delta_{i,j}^{(t)}}(d|\mathbf{z}) = \phi_{D_{i,j}^{(t)}}(-d|\mathbf{z})$ ). We then have the following Lemma.

**Lemma 2.** If a decoder having a symmetric message-update function and taking its inputs from an output-symmetric communication channel is affected by weakly symmetric deviations, its message error probability at any iteration  $t \geq 0$  is independent of the transmitted codeword.

*Proof:* Similarly to the approach used in [24, Lemma 4.90] and [9], we want to show that the probability that messages are in error is the same whether  $\mathbf{xz}$  or  $\mathbf{z}$  is received. This is the case if the faulty messages  $\mu_{i,j}^{(t)}$  have a symmetric distribution for all  $t \geq 0$  and all  $(i, j)$ .

Since the communication channel is output symmetric and since no deviations can occur before the first iteration, messages  $\mu_{i,j}^{(0)} = \nu_{i,j}^{(0)}$  have a symmetric distribution. We proceed by induction to establish the symmetry of the messages for  $t > 0$ . We start by assuming that

$$\phi_\nu \left( \nu_{i,j}^{(t)} \middle| \mathbf{y} \right) = \phi_\nu \left( x_i \nu_{i,j}^{(t)} \middle| \mathbf{z} \right) \quad (8)$$

also holds for  $t > 0$ . From the deviation model, we have that for  $t > 0$ ,

$$\mu_{i,j}^{(t)} = \nu_{i,j}^{(t)} + D_{i,j}^{(t-1)}. \quad (9)$$

To improve clarity, let us write  $\mu$  instead of  $\mu_{i,j}^{(t)}$ ,  $\nu$  instead of  $\nu_{i,j}^{(t)}$ ,  $D$  instead of  $D_{i,j}^{(t-1)}$ , and  $\Delta$  instead of  $\Delta_{i,j}^{(t-1)}$ . Using (8), (9) and Definition 4, we can write the faulty message distribution as

$$\begin{aligned} \phi_\mu (\mu | \mathbf{xz}) &= \int_{-\infty}^{\infty} \phi_\mu (\mu | \nu, \mathbf{xz}) \phi_\nu (\nu | \mathbf{xz}) d\nu \\ &= \int_{-\infty}^{\infty} \phi_D (\mu - \nu | \mathbf{xz}) \phi_\nu (x_i \nu | \mathbf{z}) d\nu \\ &= \int_{-\infty}^{\infty} \phi_\Delta (x_i (\mu - \nu) | \mathbf{z}) \phi_\nu (x_i \nu | \mathbf{z}) d\nu \end{aligned}$$

Definition 4 gives us that  $\phi_D (d | \mathbf{z}) = \phi_\Delta (d | \mathbf{z})$ , and therefore we can rewrite the equation above as

$$\begin{aligned} \phi_\mu (\mu | \mathbf{xz}) &= \int_{-\infty}^{\infty} \phi_D (x_i (\mu - \nu) | \mathbf{z}) \phi_\nu (x_i \nu | \mathbf{z}) d\nu \\ &= \int_{-\infty}^{\infty} \phi_D (x_i \mu - \nu' | \mathbf{z}) \phi_\nu (\nu' | \mathbf{z}) d\nu \\ &= \phi_\mu (x_i \mu | \mathbf{z}), \end{aligned}$$

where the second equality is obtained using the substitution  $\nu' = x_i \nu$ . Therefore,  $\mu_{i,j}^{(t)}$  has a symmetric distribution if  $\nu_{i,j}^{(t)}$  has a symmetric distribution. Finally, since the decoder's message-update function is symmetric, Lemma 1 confirms the induction hypothesis in (8).  $\blacksquare$

The last remaining step in establishing whether density evolution can be used with our decoder when affected by deviations is to determine whether the error-correction performance of a code concentrates around the cycle-free case. The property has been shown to hold in [9] (Theorems 2, 3 and 4) for an LDPC decoder affected by “wire noise” and “computation noise”. The wire noise model is similar to our deviation model, in the sense that the messages are passed through

an additive noise channel, and that the noise applied to one message is independent of the noise applied to other messages. The proof presented in [9] only relies on the fact that the wire noise applied to a given message can only affect messages that are included in the directed neighborhood of the edge where it is applied, where the graph direction refers to the direction of message propagation. This clearly also holds in the case of our deviation model, and therefore the proof is the same.

Since the message error probability is independent of the transmitted codeword, and furthermore concentrates around the cycle-free case, density evolution can be used to determine the error-correction performance of a decoder perturbed by our deviation model, as long as the deviations are weakly symmetric.

### *C. Deviation Measurements*

To construct a deviation model for a particular decoder, we first measure the deviations occurring in the test circuit that corresponds to the chosen code ensemble. The CAD workflow used to perform these measurements is described in Appendix A. The test circuit implements the one-iteration computation tree, and deviation statistics are collected using Monte-Carlo simulation.

When analyzing the decoding performance of reliable LDPC decoders, it is common to use a simplified DE that tracks a one-dimensional characterization of the message distribution, rather than the exact probability mass function. This approach is often called an ExIT chart. As mentioned in Section II-A, the belief output of an AWGN channel can be characterized exactly by a 1-D normal distribution. In a reliable decoder, a 1-D normal distribution remains an accurate approximation of the message distribution at any decoding iteration, because the variance-to-mean ratio of messages remains constant [25]. However, this is not necessarily the case in a faulty decoder. Nonetheless, we observe that the message error rate  $p_e^{(t)}$  predicted by an ExIT chart of the faulty decoder remains close to the actual  $p_e^{(t)}$  obtained using DE. This motivates us to use a 1-D input message distribution for the Monte-Carlo simulation of deviations. The advantage of this approach is that the deviation model can be constructed without prior knowledge of the iterative progress of the decoder. The detailed procedure for the Monte-Carlo simulation of deviations on the test circuit is provided in Appendix B.

We collect deviation measurements from the test circuits by inputting test vectors representing

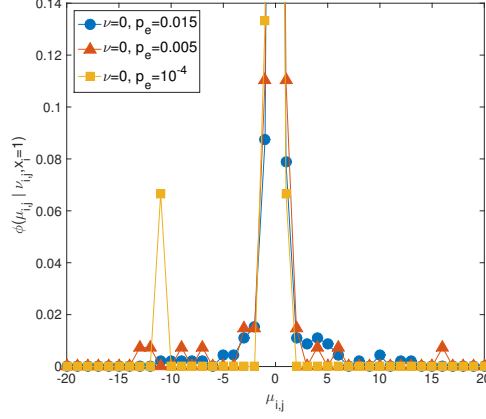


Fig. 4. Conditional distribution of faulty messages given  $\nu_{i,j}^{(t)} = 0$  and  $x_i = 1$  for some selected  $p_e^{(t)}$  values, measured on a (3,30) circuit operated at  $V_{\text{dd}} = 0.75$  V and  $T_{\text{clk}} = 3.2$  ns. The points at  $\mu_{i,j}^{(t)} = 0$  are not shown to focus on the deviations.

random codewords, and distributed according to several  $p_e^{(t)}$  values. We then normalize the data given  $x_i = 1$ , and measure  $\phi_{\mu|\nu}^{(p_e^{(t)})}(\mu_{i,j}^{(t)} | \nu_{i,j}^{(t)}, x_i = 1)$ . Finally, to obtain a weakly symmetric deviation model, we define

$$\phi_{\mu|\nu}^{(p_e^{(t)})}(\mu_{i,j}^{(t)} | \nu_{i,j}^{(t)}, x_i = -1) = \phi_{\mu|\nu}^{(p_e^{(t)})}(-\mu_{i,j}^{(t)} | -\nu_{i,j}^{(t)}, x_i = 1).$$

Fig. 4 shows examples of conditional distributions of the faulty messages measured on the test circuit, for  $\nu_{i,j}^{(t)} = 0$  and  $x_i = 1$ . We can first note that the deviations vary significantly in terms of  $p_e^{(t)}$ . We can also note that there is no sign symmetry of the deviation, and therefore that a symmetric deviation model would not be suitable. Finally, only a few  $\mu_{i,j}^{(t)}$  values have a non-zero probability. These general trends are observed in all the deviation measurements that have been performed.

Let  $p_L$  and  $p_H$  be respectively the smallest and largest  $p_e^{(t)}$  values for which the deviation has been characterized. We can generate a conditional distribution for any  $p_e^{(t)} \in [p_L, p_H]$  by interpolating from the nearest distributions that have been measured. We choose  $p_H \geq p_e^{(0)}$  to make sure that the first iteration's deviation is within the characterized range. Because messages in the decoder are saturated once they reach the largest magnitude that can be represented, the circuit's switching activity decreases as the message error probability decreases. Since timing faults cannot occur when the circuit does not switch, we can expect deviations to be equally or less likely at lower  $p_e^{(t)}$  values. Therefore, to define the deviation model for  $p_e^{(t)} < p_L$ , we make

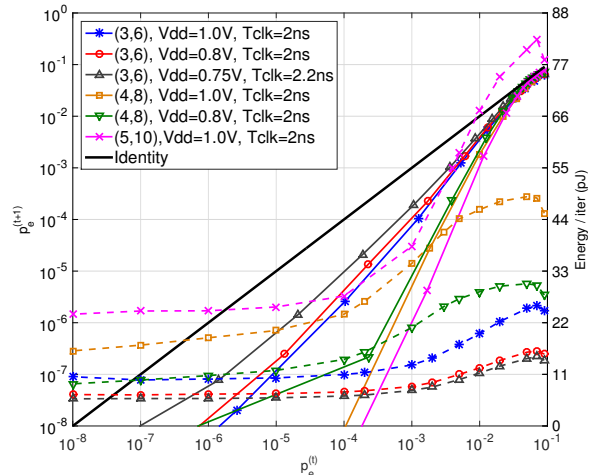


Fig. 5. Examples of projected DE and energy curves for rate 0.5 ensembles with  $d_v \in \{3, 4, 5\}$ , and  $p_e^{(0)} = 0.09$ . Energy curves are shown as dashed curves.

the pessimistic assumption that the deviation distribution remains the same as for  $p_e^{(t)} = p_L$ .

#### D. DE and Energy Curves

We evaluate the progress of the decoder affected by timing violations using quantized density evolution [26]. For the Offset Min-Sum algorithm, a DE iteration can be split into the following steps: 1-a) evaluating the distribution of the CN minimum, 1-b) evaluating the distribution of the CN output, after subtracting the offset, 2) evaluating the distribution of the ideal VN-to-CN message, and 3) evaluating the distribution of the faulty VN-to-CN messages. Step 1-a is given in [14], while the others are straightforward. In the context of DE, we write the message distribution as  $\boldsymbol{\pi}^{(t)} = \phi(\mu_{i,j}^{(t)} | x_i = 1)$ , and the channel output distribution as  $\boldsymbol{\pi}^{(0)} = \phi(\nu_i^{(0)} | x_i = 1)$ . We write a DE iteration as  $\boldsymbol{\pi}^{(t+1)} = f_\gamma(\boldsymbol{\pi}^{(t)}, \boldsymbol{\pi}^{(0)})$ .

The energy consumption is measured on the test circuit using a 1-D input message distribution, and therefore it is best described in terms of the message error probability. We write the energy function as  $c_\gamma(p_e^{(t)})$ . To display  $f_\gamma(\phi(\mu_{i,j}^{(t)} | x_i = 1))$  and  $c_\gamma(p_e^{(t)})$  on the same plot, we project  $\phi(\mu_{i,j}^{(t)} | x_i = 1)$  onto the message error probability space.

Several regular code ensembles were evaluated, with rates  $\frac{1}{2}$  and  $\frac{9}{10}$ . Fig. 5 shows examples of projected DE curves and energy curves for rate- $\frac{1}{2}$  code ensembles with  $d_v \in \{3, 4, 5\}$  and various operating conditions. The energy is measured as described in Appendix A and corresponds to

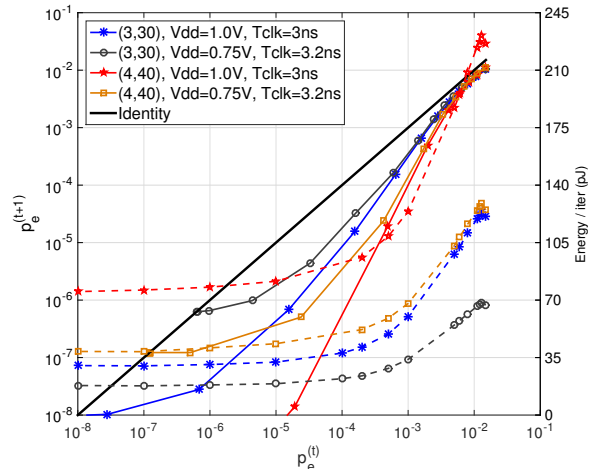


Fig. 6. Examples of projected DE and energy curves for the (3, 30) and (4, 40) ensembles (rate 0.9), with  $p_e^{(0)} = 0.015$ . Energy curves are shown as dashed curves.

one complete decoding iteration performed with the test circuit, requiring  $d_v$  uses of the test circuit. The nominal operating condition is  $V_{dd} = 1.0$  V,  $T_{clk} = 2.0$  ns and therefore these curves correspond to a reliable implementation. With a reliable implementation, these ensembles have a channel threshold of  $p_e^{(0)} \leq 0.12$  for the (3, 6) ensemble,  $p_e^{(0)} \leq 0.11$  for (4, 8), and  $p_e^{(0)} \leq 0.09$  for (5, 10). We use  $p_e^{(0)} = 0.09$  for all the curves shown in Fig. 5 to allow comparing the ensembles. As can be expected, a larger variable node degree results in faster convergence towards zero error rate, and it is natural to ask whether this property might provide greater fault tolerance and ultimately better energy efficiency. However, we can see that the energy per iteration increases rapidly as  $d_v$  increases, and our energy optimization results show that for minimizing energy or EDP it is best to choose the ensemble with the smallest possible variable node degree.

Fig. 6 is a similar plot for the (3, 30) and (4, 40) ensembles. The channel threshold of both ensembles is approximately  $p_e^{(0)} \leq 0.019$ . For these curves, the nominal operating condition is  $V_{dd} = 1.0$  V and  $T_{clk} = 3$  ns. As we can see, the energy consumption per iteration of the (4, 40) decoder is roughly double that of the (3, 30) decoder. We note that in the case of the (3, 30) ensemble, the reliable decoder stops making progress at an error probability of approximately  $10^{-8}$ . This floor is the result of the message saturation limit chosen for the circuit.

## V. ENERGY OPTIMIZATION

### A. Design Parameters

As in a standard LDPC code-decoder design, the first parameter to be optimized is the choice of code ensemble. In this paper we restrict the discussion to regular codes, and therefore we need only to choose a degree pair  $(d_v, d_c)$ , where  $R = 1 - d_v/d_c$  is the design rate of the code. For a fixed  $R$ , we can observe that both the energy consumption and the circuit area of the decoding circuit grow rapidly with  $d_v$ , and therefore it is only necessary to consider a few of the lowest  $d_v$  values.

Besides the choice of ensemble, we are interested in finding the optimal choice of operating parameters for the quasi-synchronous circuit. We consider here the supply voltage ( $V_{dd}$ ) and the clock period ( $T_{clk}$ ). Generally speaking, the supply voltage affects the energy consumption, while the clock period affects the decoding time, or latency. The energy and latency are also affected by the choice of code ensemble, since the number of operations to be performed depends on the node degrees. The operating parameters of a decoder are denoted as a vector  $\gamma = [V_{dd}, T_{clk}]$ .

The decoding of LDPC codes proceeds in an iterative fashion, and it is therefore possible to adjust the operating parameters on an iteration-by-iteration basis. In practice, this could be implemented in various ways, for example by using a pipelined sequence of decoder circuits, where each decoder is responsible for only a portion of the decoding iterations. It is also possible to rapidly vary the clock frequency of a given circuit by using a digital clock divider circuit [27]. We denote by  $\bar{\gamma}$  the sequence of parameters used at each iteration throughout the decoding, and we use  $\bar{\gamma} = [\gamma_1^{N_1}, \gamma_2^{N_2}, \dots]$  to denote a specific sequence in which the parameter vector  $\gamma_1$  is used for the first  $N_1$  iterations, followed by  $\gamma_2$  for the next  $N_2$  iterations, and so on.

### B. Objective

The performance of the LDPC code and of its decoder can be described by specifying a vector  $\mathbf{P} = (p_e^{(0)}, p_{res}, T_{dec})$ , where  $p_e^{(0)}$  is the output error rate of the communication channel,  $p_{res}$  the residual error rate of VN-to-CN messages when the decoder terminates, and  $T_{dec}$  the expected decoding latency.

The decoder's performance  $\mathbf{P}$  and energy consumption  $E$  are controlled by  $\bar{\gamma}$ . The energy minimization problem can be stated as follows. Given a performance constraint  $\mathbf{P} = (a, b, c)$ ,

we wish to find the value of  $\bar{\gamma}$  that minimizes  $E$ , subject to  $p_e^{(0)} \geq a$ ,  $p_{\text{res}} \leq b$ ,  $T_{\text{dec}} \leq c$ . As in the standard DE method, we propose to use the code’s computation tree as a proxy for the entire decoder, and furthermore to use the energy consumption of the test circuit described in Appendix B as the optimization objective. To be able to replace the energy minimization of the complete decoder with the energy minimization of the test circuit, we make the following assumptions:

- 1) The ordering of the energy consumption is the same for the test circuit and for the complete decoder, that is, for any  $\gamma_1$  and  $\gamma_2$ ,  $E_{\text{TEST}}(\gamma_1) \leq E_{\text{TEST}}(\gamma_2)$  implies  $E_{\text{DEC}}(\gamma_1) \leq E_{\text{DEC}}(\gamma_2)$ , where  $E_{\text{TEST}}(\gamma)$  and  $E_{\text{DEC}}(\gamma)$  are respectively the energy consumption of the test circuit and of the complete decoder when using parameter  $\gamma$ .
- 2) The average message error rate in the test circuit and in the complete decoder is the same for all decoding iterations.
- 3) The latency of the complete decoder is proportional to the latency of the test circuit, that is, if  $T_{\text{dec}}(\gamma)$  is the latency measured using the test circuit with parameter  $\gamma$ , the latency of the complete decoder is given by  $\beta T_{\text{dec}}(\gamma)$ , where  $\beta$  does not depend on  $\gamma$ .

Assumption 1 is reasonable because the test circuit is very similar to a computation unit used in the complete decoder. The difference between the two is that the test circuit only instantiates one full VNP, the remaining  $(d_c - 1)$  VNPs being reduced to only their “front” part (as seen in Fig. 7), whereas the complete decoder has  $d_c$  full VNPs for every CNP. Assumption 2 is the standard DE assumption, which is reasonable for sufficiently long codes. Finally, it is possible for the clock period to be slower in the complete decoder, because the increased area could result in longer interconnections between circuit blocks. Even if this is the case, the interconnect length only depends on the area of the complete decoder, which is not affected by the parameters we are optimizing, and hence  $\beta$  does not depend on  $\gamma$ .

Clearly, if Assumption 1 holds and the performance of the test circuit is the same as the performance of the complete decoder, then the solution of the energy minimization is also the same. However, it is not obvious that the performance of the complete decoder will be identical to the performance of the test circuit. The performance is composed of the three components  $(p_e^{(0)}, p_{\text{res}}, T_{\text{dec}})$ . The channel error rate  $p_e^{(0)}$  does not depend on the decoder and is clearly the same in both cases. Because of Assumption 2, the complete decoder can achieve the same residual

error rate as the test circuit when  $p_e^{(0)}$  is the same. The latencies measured on the test circuit and on the complete decoder are not necessarily the same, but if Assumption 3 holds, and if we assume that the constant  $\beta$  is known, then we can find the solution to the energy minimization of the complete decoder subject to constraints  $(p_e^{(0)}, p_{\text{res}}, T_{\text{dec}})$  by instead minimizing the energy of the test circuit with constraints  $(p_e^{(0)}, p_{\text{res}}, T_{\text{dec}}/\beta)$ .

We also consider another interesting optimization problem. It is well known that for a fixed degree of parallelism, processing speed (represented here by  $T_{\text{dec}}$ ) and energy consumption have a proportional relationship, which is observed both in the physical energy limit stemming from Heisenberg’s uncertainty principle [28], as well as in practical CMOS circuits [29]. In situations where both throughput normalized to area and low energy consumption are desired, optimizing the product of energy and latency or *energy-delay product* (EDP) for a fixed circuit area can be a better objective. In that case the performance constraint is stated in terms of  $\mathbf{P} = (p_e^{(0)}, p_{\text{res}})$ , and the optimization problem becomes the following: given a performance constraint  $\mathbf{P} = (a, b)$ , minimize  $E(\bar{\gamma}) \cdot T_{\text{dec}}(\bar{\gamma})$  subject to  $p_e^{(0)} \geq a$ ,  $p_{\text{res}} \leq b$ , and a fixed circuit area.

### C. Dynamic Programming

To solve the iteration-by-iteration energy and EDP minimization problems stated above, we adapt the “Gear-Shift” dynamic programming approach proposed in [15]. The original method relies on the fact that the message distribution has a 1-D characterization, which is chosen to be the error probability. By quantizing the error probability space, a trellis graph can be constructed in which each node is associated with a pair  $(p_e^{(t)}, t)$ . A particular choice of  $\bar{\gamma}$  corresponds to a path  $P$  through the graph, and the optimization is transformed into finding the least expensive path that starts from the initial state  $(p_e^{(0)}, 0)$  and reaches any state  $(p_e^{(t)}, t)$  such that  $p_e^{(t)} \leq p_{\text{res}}$  and the latency constraint is satisfied, if there is one.

However, in the case of a faulty decoder, we want to evaluate the decoder’s progress by tracking a complete message distribution using DE, rather than simply tracking the message error probability. In this case, the Gear-Shift method can be used as an approximate solver by projecting the message distribution  $\pi^{(t)} = \phi(\mu_{i,j}^{(t)} | x_i = 1)$  onto the error probability space. We refer to this method as DE-Gear-Shift. Any path through the graph is evaluated by performing DE on the entire path using exact distributions, but the performance and cost of two paths are compared in the projection space. As a result, the solutions that are found are not guaranteed to

be optimal, but they are guaranteed to accurately represent the progress of the decoder.

In the DE-Gear-Shift method, a path  $P$  is a sequence of states  $\{\pi^{(t)}\}$ . As in the original Gear-Shift method, any sequence of decoder parameters  $\bar{\gamma}$  corresponds to a path. We denote the projection of a state into the error probability space as  $p_e^{(t)} = \Theta(\pi^{(t)})$ . To each path  $P$ , we associate an energy cost  $E_P$  and a latency cost  $T_P$ . A path ending at a state  $\pi^{(t)}$  can be extended with one additional decoding iteration using parameter  $\gamma$  by evaluating one DE iteration to obtain  $\pi^{(t+1)} = f_\gamma(\pi^{(t)}, \pi^{(0)})$ . Performing this additional iteration adds an energy cost  $c_\gamma(p_e^{(t)}, p_e^{(0)})$  and a latency cost  $T_\gamma$  to the path's cost.

A path  $P$  with cost  $C_P$  is said to *dominate* another path  $P'$  with cost  $C_{P'}$  if all the following conditions hold: 1) an ordering exists between  $C_P$  and  $C_{P'}$ , 2)  $C_P \leq C_{P'}$ , 3)  $\Theta(\pi_P) \leq \Theta(\pi_{P'})$ , where  $\pi_P$  denotes the last state reached by path  $P$ . The search for the least expensive path is performed breadth-first. After each traversal of the graph, any path that is dominated by another is discarded, greatly reducing the number of paths that must be evaluated.

When optimizing EDP, we can define the overall cost of a path  $C_P$  as  $C_P = E_P \cdot T_P$ . Because  $C_P$  is one-dimensional, an ordering always exists between the costs, and more paths can be discarded. However, when optimizing energy under a latency constraint, the cost of a path must include a latency dimension, and we have  $C_P = (E_P, T_P)$ . In this case, there is no total order on path costs. Nonetheless, an ordering exists between the costs of paths  $P$  and  $P'$  if  $(E_P \geq E_{P'} \wedge T_P \geq T_{P'}) \vee (E_P \leq E_{P'} \wedge T_P \leq T_{P'})$ , and in that case the discarding rule can be applied.

In practice, we might be interested in finding parameter sequences that have other desirable properties beyond minimal energy or EDP. For example, if the decoder is implemented as a pipelined sequence of decoders, it can be desirable to favor solutions that do not require the decoder to switch its parameters too often. We can find good approximate solutions by adding a penalty to  $E_P$  when the algorithm used in the current and next steps is different.

#### D. Results

We use DE-Gear-Shift to find good parameter sequences  $\bar{\gamma}$  for several regular ensembles with rates  $\frac{1}{2}$  and  $\frac{9}{10}$ . The parameter space  $\Gamma$  consists of  $(V_{\text{dd}}, T_{\text{clk}})$  points with  $V_{\text{dd}}$  from 0.70 V to 1.0 V in steps of 0.05 V and several  $T_{\text{clk}}$  values depending on  $V_{\text{dd}}$ , in steps of 0.1 ns. The standard and quasi-synchronous decoders use the same circuits. As part of our best effort to design a good

TABLE I  
ENERGY AND EDP OPTIMIZATION RESULTS.

Code family	Nom. $T_{\text{clk}}$	Norm. area †	$p_e^{(0)}$	$p_{\text{res}}$	Latency [ns]	Standard		Quasi-synchronous	
						Energy [pJ]	EDP [nJ · ns]	Best energy [pJ]	Best EDP [nJ · ns]
(3,6)	2.0 ns	1.066	0.12 <sup>‡</sup>	$10^{-8}$	198	750	149	575 (-23%)	114 (-23%)
			0.09	$10^{-8}$	66	185	13.5	135 (-34%)	8.8 (-35%)
(4,8)	2.0 ns	1.44	0.09	$10^{-8}$	72	394	28.4	299 (-24%)	21.2 (-25%)
(3,30)	3.0 ns	1.099	0.019 <sup>‡</sup>	$10^{-8}$	252	<b>2650</b>	668	<b>1816</b> (-31%)	437 (-35%)
	2.5 ns	1.135	0.019 <sup>‡</sup>	$10^{-8}$	210	2748	<b>577</b>	2004 (-27%)	<b>420</b> (-27%)
	3.0 ns	1.099	0.015	$10^{-8}$	117	<b>918</b>	107	<b>588</b> (-36%)	66.1 (-38%)
	2.5 ns	1.135	0.015	$10^{-8}$	97.5	972	<b>95</b>	653 (-33%)	<b>62.5</b> (-34%)
(4,40)	3.0 ns	1.522	0.015	$10^{-8}$	108	1456	157	897 (-38%)	95 (-40%)

† Cell area divided by the minimal area of the smallest decoder having the same code rate. ‡ Approx. threshold.

standard circuit, in the case of the (3, 30) decoder we present results for two circuits synthesized with different nominal  $T_{\text{clk}}$  values. The standard circuit has a lower energy consumption using the first circuit, while it has a lower EDP with the second circuit.

We first run the DE-Gear-Shift solver without any path penalties to obtain the best possible parameter sequences, for both the energy and the EDP objectives. We also noticed that in some cases, adding a small algorithm change penalty allows to discover slightly better sequences. Note that when the objective is EDP, there is no constraint on latency. These results are summarized in Table I. Overall, we see that significant gains are possible while achieving the same channel noise, latency, and residual error requirements. The results confirm that among these regular ensembles, increasing  $d_v$  causes a significant increase in the decoding energy, both for a standard decoder and for a quasi-synchronous decoder, in addition to an increase in circuit area. Furthermore, we see that much more energy is required when operating the decoder close to the channel threshold. Nonetheless, significant energy or EDP gains are still possible close to the threshold, although the gains increase with a better channel.

By applying a cost penalty to parameter switches, it is possible to find parameter sequences with few switches, without a large increase in cost. For example, for a (3, 6) decoder starting at  $p_e^{(0)} = 0.09$ , two  $(V_{\text{dd}}, T_{\text{clk}})$  pairs are sufficient to provide a 33% EDP improvement, using  $\bar{\gamma} =$

$[[0.8 \text{ V}, 2.1 \text{ ns}]^8, [1.0 \text{ V}, 1.4 \text{ ns}]^3]$ . The average deviation probability in that schedule ranges from 1.6% to 7.2%. In the case of a (3, 30) decoder, at  $p_e^{(0)} = 0.015$ , the sequence  $\bar{\gamma} = [[0.8 \text{ V}, 3 \text{ ns}]^{12}, [1.0 \text{ V}, 2.5 \text{ ns}]^9]$  provides a 36% EDP improvement, with average deviation probabilities from 0 to 0.9%. For a (4, 40) decoder, the single-parameter sequence  $\bar{\gamma} = [[0.8 \text{ V}, 2.8 \text{ ns}]^9]$  provides a 39% EDP improvement, with average deviation probabilities from 0.4 to 3%.

## VI. CONCLUSION

We presented a method for the design of synchronous circuit implementations of signal processing algorithms that permits timing violations without the need for hardware compensation. The method uses small test circuits to obtain accurate deviation statistics and energy estimation. We introduced a model for the deviations occurring in LDPC decoder circuits affected by timing faults that is sufficiently general to accurately represent the circuit behavior, while still being memoryless. In addition, we showed that in order to use density evolution to predict the performance of the faulty decoder, it is sufficient for the deviation model to have a weak symmetry property, which is more general than previously proposed sufficient properties.

We then presented an approximate optimization method called DE-Gear-Shift to find sequences of circuit operating parameters that minimize the energy or the energy-delay product. The method is similar to the previously proposed Gear-Shift method, but relies on density evolution rather than EXIT charts to evaluate the average iterative progress of the decoder. Our results show that the best energy or EDP reduction is achieved by operating the circuit with a large number of timing violations (often with an average deviation rate above 1%). Furthermore, important savings can be achieved with few parameter switches, and without any compromise on circuit area or decoding performance.

## APPENDIX A

### CAD WORKFLOW

To make the characterization as accurate as possible, we measure the deviations and the energy consumption directly on optimized circuit models generated by a commercial synthesis tool (Cadence Encounter [30]). We use TSMC’s 65 nm process with the *tcbn65gplus* cell library [31]. In order to provide a fair assessment of the improvements provided by the quasi-synchronous circuit, we first synthesize a *benchmark* circuit that represents a best effort at

optimizing the metric of interest, for example energy consumption. Since we do not have a specific throughput constraint for the design, we synthesize the benchmark circuit at the standard supply voltage of the library ( $V_{dd} = 1.0V$ ), while the clock period is chosen as small as possible without causing a degradation of the target metric. Second, we synthesize a *nominal* circuit that will serve as the basis for the quasi-synchronous design. In this work, we use a standard synthesis algorithm for the nominal circuit, and in all the cases that we report on, the nominal and the benchmark circuits are actually the same. Using a standard synthesis method for the nominal circuit allows using off-the-shelf tools, but is not ideal since the objective of a standard synthesis algorithm (to make all paths only as fast as the clock period) differs from the objective pursued when some timing violations are permitted. For example, results in [32] show that the power consumption of a circuit can be reduced by up to 32% when the gate-sizing optimization takes into account the frequency at which the clock constraint can be violated. Therefore it is possible that our results could be improved by using a more specialized synthesis algorithm.

Once the circuit is synthesized, we perform a static timing analysis of the gate-level model at various supply voltages. All timing analyses (including at the nominal supply) are performed using timing libraries generated by the Cadence Encounter Library Characterization tool. We then use this timing information in a functional simulation of the gate-level circuit to observe the dynamic effect of path delay variations and measure the deviation statistics. Any source of delay variation that can be simulated can be studied, but in this paper we focus on variations due to path activation, that is the variations in delay caused by the different propagation times required by different input transitions. Note that other methods could be used to obtain the propagation delays, such as the method described in [33] based on analytical models. In addition to speeding up the characterization, such methods allow considering the effect of process variations.

Power estimation is performed by collecting switching activity data in the functional simulation and using the power estimation engine in Cadence Encounter. However, because the circuit is operated in a quasi-synchronous manner, the clock period used to run the circuit is not necessarily the same as the nominal clock period. When that is the case, the power estimation generated by the synthesis tool cannot be used directly. First, the switching activity recorded during the functional simulation must be scaled so that it corresponds to the nominal clock period. The tool's power estimation then reports the dynamic power  $P_{dyn}$  and the static power  $P_{stat}$ . The dynamic energy consumed during one clock cycle does not depend on the clock period, whereas

the static energy does. Therefore, the total energy consumed during one cycle by the quasi-synchronous circuit is given by  $E_{\text{cycle}} = P_{\text{dyn}}T_{\text{clk,nom}} + P_{\text{stat}}T_{\text{clk}}$ , where  $T_{\text{clk,nom}}$  is the nominal clock period and  $T_{\text{clk}}$  is the actual clock period used to run the circuit.

## APPENDIX B

### TEST CIRCUIT MONTE-CARLO SIMULATION

A suitable test circuit for a row-layered decoder architecture consists in implementing a single check node processor, as well as the necessary logic taken from the variable node processor block to send  $d_v$  messages to the CNP, and receive one message from the CNP. This test circuit is shown in Fig. 7. It re-uses logic blocks that are found in the complete decoder, ensuring the accuracy of the deviation and energy measurements, and minimizing design time. At any given clock cycle, a *VNP front* block is mapped to a particular VN  $i$ . Each *VNP front* block takes as input the previous belief total of that VN, denoted  $\Lambda'_i$ , and the previous CN-to-VN message for the current layer  $\ell$ , denoted  $\lambda_i^{(t-1,\ell)}$ . The previous belief total is defined as

$$\Lambda'_i = \begin{cases} \Lambda_i^{(t-1,L)} & \text{if } \ell = 1, \\ \Lambda_i^{(t,\ell-1)} & \text{if } \ell > 1. \end{cases}$$

As part of the proposed design framework, we require that the input and output of the test circuit be accurately modeled as stationary processes when the test circuit is used in the final system. In this case, since the function implemented by the circuit is memoryless, the stationarity of the output process is implied by the stationarity of the input process. To determine whether the circuit's input can realistically be modeled as a stationary process (with respect to the clock cycles), we must consider the way the circuit is used when instantiated in the complete decoder. The input of a given *VNP front* is determined by the VN it is associated with, as well as the iteration and layer indices. If we assume that the code graph is cycle free, the messages sent by all VNs at iteration  $t$  and layer  $\ell$  are i.i.d. Therefore, when a VNP is assigned to process a sequence of distinct VNs belonging to the same  $(t, \ell)$ , its inputs can be represented by an i.i.d. process. If the number of CNPs instantiated in the decoder is significantly less than  $m/L$ , then for most cycles the current and the next inputs of a VNP do belong to the same  $(t, \ell)$ , making this a reasonable approximation.

To perform the Monte-Carlo simulation, a *VNP front* circuit block with index  $i$  must send a message  $\mu_i^{(t)}$ , randomly generated according to a 1-D normal distribution with error probability

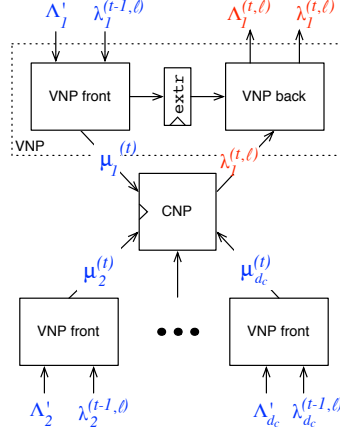


Fig. 7. Block diagram of the test circuit.

$p_e^{(t)}$ . However, the only inputs that are controllable are  $\Lambda'_i$  and  $\lambda_i^{(t-1, \ell)}$ . To simplify the Monte-Carlo simulation, we disregard the true distribution of  $\lambda_i^{(t-1, \ell)}$ , and simply pick a 1-D normal distribution with a parameter chosen such that  $\mu_i^{(t)}$  has the desired distribution. We also introduce another simplification: we assume that messages received at a VN only modify the total belief at the end of the iteration, as would be the case when using a flooding schedule. As a result, the messages  $\mu_i^{(t, \ell)}$  are identically distributed with error rate parameter  $p_e^{(t)}$  for all  $\ell$ . Note that these simplifications are not necessary, and they could be removed at the cost of a slightly more cumbersome Monte-Carlo simulation.

We have that  $\Lambda'_i = \mu_i^{(t, \ell)} + \lambda_i^{(t-1, \ell)}$ . On a cycle-free graph,  $\mu_i^{(t, \ell)}$  and  $\lambda_i^{(t-1, \ell)}$  are independent, but naturally  $\Lambda'_i$  and  $\lambda_i^{(t-1, \ell)}$  are not. Therefore, we generate  $\mu_i^{(t, \ell)}$  and  $\lambda_i^{(t-1, \ell)}$ , sum them to obtain  $\Lambda'_i$ , and then discard  $\mu_i^{(t, \ell)}$ . By definition, the distribution of  $\mu_i^{(t, \ell)}$  has a mean of  $\rho^{(t)}$ , and since we assume that total beliefs are updated as if using a flooding schedule, we have

$$\mu_i^{(t, \ell)} = \lambda_i^{(t-1, 1)} + \dots + \lambda_i^{(t-1, \ell-1)} + \lambda_i^{(t-1, \ell+1)} + \dots + \lambda_i^{(t-1, d_v)}. \quad (10)$$

Messages belonging to the same iteration are i.i.d., and therefore the mean of  $\lambda_i^{(t-1, \ell)}$  is given by  $\rho^{(t)}/(d_v - 1)$ .

In the test circuit, the VNP with index 1 (shown at the top of Fig. 7) is at the root of the computation tree. To complete the DE iteration, we want to measure

$$\mu_1^{(t+1, d_v)} = \lambda_1^{(t, 1)} + \lambda_1^{(t, 2)} + \dots + \lambda_1^{(t, d_v-1)}. \quad (11)$$

To achieve this, we set  $\Lambda_1^{(t-1,L)} \leftarrow 0$  and  $\lambda_1^{(t-1,\ell)} \leftarrow 0$  for all  $\ell$ . We then have  $\mu^{(t+1,d_v)} = \Lambda_1^{(t,d_v-1)}$ , that is the next extrinsic message corresponds directly to the circuit's total belief output after it has been used  $d_v - 1$  times.

#### ACKNOWLEDGEMENTS

The authors wish to thank CMC Microsystems for providing access to the Cadence tools and TSMC 65nm CMOS technology, and Gilles Rust for advice on Cadence tools and cell library characterization.

#### REFERENCES

- [1] S. Ghosh and K. Roy, "Parameter variation tolerance and error resiliency: New design paradigm for the nanoscale era," *Proc. of the IEEE*, vol. 98, no. 10, pp. 1718–1751, Oct. 2010.
- [2] R. Dreslinski, M. Wieckowski, D. Blaauw, D. Sylvester, and T. Mudge, "Near-threshold computing: Reclaiming moore's law through energy efficient integrated circuits," *Proc. of the IEEE*, vol. 98, no. 2, pp. 253–266, Feb. 2010.
- [3] T. Austin, V. Bertacco, D. Blaauw, and T. Mudge, "Opportunities and challenges for better than worst-case design," in *Proc. of the 2005 Asia and South Pacific Design Automation Conf.*, 2005, pp. 2–7.
- [4] K. Bowman, J. Tschanz, N. S. Kim, J. Lee, C. Wilkerson, S.-L. Lu, T. Karnik, and V. De, "Energy-efficient and metastability-immune resilient circuits for dynamic variation tolerance," *IEEE J. of Solid-State Circuits*, vol. 44, no. 1, pp. 49–63, Jan. 2009.
- [5] S. Das, C. Tokunaga, S. Pant, W.-H. Ma, S. Kalaiselvan, K. Lai, D. Bull, and D. Blaauw, "RazorII: In situ error detection and correction for PVT and SER tolerance," *IEEE J. of Solid-State Circuits*, vol. 44, no. 1, pp. 32–48, Jan. 2009.
- [6] R. Hegde and N. R. Shanbhag, "Energy-efficient signal processing via algorithmic noise-tolerance," in *Proc. 1999 Int. Symp. on Low Power Electronics and Design*, Aug. 1999, pp. 30–35.
- [7] B. Shim, S. Sridhara, and N. Shanbhag, "Reliable low-power digital signal processing via reduced precision redundancy," *IEEE Trans. on VLSI Systems*, vol. 12, no. 5, pp. 497–510, May 2004.
- [8] Y. Liu, T. Zhang, and K. Parhi, "Computation error analysis in digital signal processing systems with overscaled supply voltage," *IEEE Trans. on VLSI Systems*, vol. 18, no. 4, pp. 517–526, Apr. 2010.
- [9] L. Varshney, "Performance of LDPC codes under faulty iterative decoding," *IEEE Trans. Inf. Theory*, vol. 57, no. 7, pp. 4427–4444, Jul. 2011.
- [10] F. Leduc-Primeau and W. J. Gross, "Faulty Gallager-B decoding with optimal message repetition," in *Proc. 50th Allerton Conf. on Communication, Control, and Computing*, Oct. 2012.
- [11] S. M. S. Tabatabaei Yazdi, H. Cho, and L. Dolecek, "Gallager B decoder on noisy hardware," *IEEE Trans. Commun.*, vol. 61, no. 5, pp. 1660–1673, May 2013.
- [12] C.-H. Huang, Y. Li, and L. Dolecek, "Gallager B LDPC decoder with transient and permanent errors," *IEEE Trans. Commun.*, vol. 62, no. 1, pp. 15–28, Jan. 2014.
- [13] C. Ngassa, V. Savin, and D. Declercq, "Min-sum-based decoders running on noisy hardware," in *IEEE Global Communications Conf. (GLOBECOM)*, Dec. 2013, pp. 1879–1884.

- [14] A. Balatsoukas-Stimming and A. Burg, "Density evolution for min-sum decoding of LDPC codes under unreliable message storage," *IEEE Commun. Lett.*, vol. 18, no. 5, pp. 849–852, May 2014.
- [15] M. Ardakani and F. R. Kschischang, "Gear-shift decoding," *IEEE Trans. Commun.*, vol. 54, no. 7, pp. 1235–1242, Jul. 2006.
- [16] K. Cushon, C. Leroux, S. Hemati, S. Mannor, and W. Gross, "A min-sum iterative decoder based on pulsewidth message encoding," *IEEE Trans. Circuits Syst. II, Exp. Briefs*, vol. 57, no. 11, pp. 893–897, Nov. 2010.
- [17] C. Roth, P. Meinerzhagen, C. Studer, and A. Burg, "A 15.8 pJ/bit/iter quasi-cyclic LDPC decoder for IEEE 802.11n in 90 nm CMOS," in *2010 IEEE Asian Solid State Circuits Conf.*, Nov. 2010, pp. 1–4.
- [18] Y. Sun, G. Wang, and J. Cavallaro, "Multi-layer parallel decoding algorithm and VLSI architecture for quasi-cyclic LDPC codes," in *IEEE Int. Symp. on Circuits and Systems*, May 2011, pp. 1776–1779.
- [19] A. Cevrero, Y. Leblebici, P. Jenne, and A. Burg, "A 5.35 mm<sup>2</sup> 10GBASE-T ethernet LDPC decoder chip in 90nm CMOS," in *Proc. IEEE Asian Solid-State Circuits Conf.*, Nov. 2010.
- [20] C.-L. Wey, M.-D. Shieh, and S.-Y. Lin, "Algorithms of finding the first two minimum values and their hardware implementation," *IEEE Trans. Circuits Syst. I, Reg. Papers*, vol. 55, no. 11, pp. 3430–3437, Dec. 2008.
- [21] B. Sedighi, N. P. Anthapadmanabhan, and D. Suvakovic, "Timing errors in LDPC decoding computations with overscaled supply voltage," in *Proc. 2014 Int. Symp. on Low Power Electronics and Design*, Aug. 2014, pp. 201–206.
- [22] E. Dupraz, D. Declercq, B. Vasic, and V. Savin. (2014) Analysis and design of finite alphabet iterative decoders robust to faulty hardware. [Online]. Available: <http://arxiv.org/abs/1410.2291>
- [23] T. J. Richardson and R. L. Urbanke, "The capacity of low-density parity-check codes under message-passing decoding," *IEEE Trans. Inf. Theory*, vol. 47, no. 2, pp. 599–618, 2001.
- [24] T. Richardson and R. Urbanke, *Modern Coding Theory*. Cambridge University Press, 2008.
- [25] M. Ardakani and F. Kschischang, "A more accurate one-dimensional analysis and design of irregular LDPC codes," *IEEE Trans. Commun.*, vol. 52, no. 12, pp. 2106–2114, Dec. 2004.
- [26] S.-Y. Chung, J. David Forney, T. J. Richardson, and R. Urbanke, "On the design of low-density parity-check codes within 0.0045dB of the Shannon limit," *IEEE Commun. Lett.*, vol. 5, no. 2, pp. 58–60, Feb. 2001.
- [27] T. Fischer, J. Desai, B. Doyle, S. Naffziger, and B. Patella, "A 90-nm variable frequency clock system for a power-managed titanium architecture processor," *IEEE J. Solid-State Circuits*, vol. 41, no. 1, pp. 218–228, Jan. 2006.
- [28] S. Lloyd, "Ultimate physical limits to computation," *Nature*, vol. 406, no. 6799, pp. 1047–1054, Aug. 2000.
- [29] R. Gonzalez and M. Horowitz, "Energy dissipation in general purpose microprocessors," *IEEE J. Solid-State Circuits*, vol. 31, no. 9, pp. 1277–1284, Sep. 1996.
- [30] Cadence Design Systems Inc., "Encounter digital implementation system." [Online]. Available: [http://www.cadence.com/products/di/edi\\_system](http://www.cadence.com/products/di/edi_system)
- [31] *TCBN65GPLUS TSMC 65nm Core Library Databook*, Taiwan Semiconductor Manufacturing Company, Ltd.
- [32] A. Kahng, S. Kang, R. Kumar, and J. Sartori, "Slack redistribution for graceful degradation under voltage overscaling," in *Proc. 15th Asia and South Pacific Design Automation Conference (ASP-DAC)*, Jan. 2010, pp. 825 –831.
- [33] A. Pirbadian, M. Khairy, A. Eltawil, and F. Kurdahi, "State dependent statistical timing model for voltage scaled circuits," in *IEEE Intl Symp. on Circuits and Systems (ISCAS)*, Jun. 2014, pp. 1432–1435.